

# Optical and infrared polarimetry of the transient LMXB Centaurus X-4 in quiescence<sup>★</sup>

M. C. Baglio<sup>1,2,3</sup>, P. D'Avanzo<sup>1</sup>, S. Campana<sup>1</sup>, and S. Covino<sup>1</sup>

<sup>1</sup> INAF, Osservatorio Astronomico di Brera, via E. Bianchi 46, 23807 Merate (Lc), Italy  
e-mail: cristina.baglio@brera.inaf.it

<sup>2</sup> Università degli Studi di Milano, Dipartimento di Fisica, via Celoria 16, 20133 Milano, Italy

<sup>3</sup> Università dell'Insubria, Dipartimento di Fisica, via Valleggio 11, 22100 Como, Italy

Received 8 January 2014 / Accepted 13 April 2014

## ABSTRACT

**Aims.** We present the first optical and infrared polarimetric study of the low-mass transient X-ray binary Centaurus X-4 during its quiescent phase. This work aims to search for an intrinsic linear polarisation component in the system emitted radiation that might be due to, e.g., synchrotron emission from a compact jet, or to Thomson scattering with free electrons in an accretion disc.

**Methods.** Multiband (*BVRI*) optical polarimetric observations were obtained over two nights in 2008 at the ESO La Silla 3.6 m telescope, equipped with the EFOSC2 instrument used in polarimetric mode. These observations cover about the 30% of the 15.1 h orbital period. We obtained *J*-band observations in 2007 with the NICS instrument on the Telescopio Nazionale *Galileo* (TNG) at La Palma, for 1 h total of observations.

**Results.** We obtained  $3\sigma$  upper limits to the polarisation degree in all of the optical bands, with the most constraining limit being in the *I*-band, where  $P_1 < 0.5\%$ . We have noticed no significant phase-correlated variability in any of the filters. The *J*-band observations provided a 6% upper limit on the polarisation level.

**Conclusions.** The constraining upper limits on the polarisation in the optical (above all in the *I*-band), allowed us to estimate the contribution of the possible emission of a relativistic particles jet to the total system radiation to be less than 10%. This is in agreement with the observation of a spectral energy distribution typical of a single black body of a K spectral type main-sequence star irradiated from the compact object, without any significant additional component in the infrared. Because of the low S/N it was not possible to investigate the possible dependency of the polarisation degree from the wavelength, which could be suggestive of polarisation induced by Thomson scattering of radiation with free electrons in the outer part of the accretion disc. Observations with higher S/N are required to examine this hypothesis in depth, searching for significant phase-correlated variability.

**Key words.** stars: jets – stars: neutron – X-rays: binaries – polarization

## 1. Introduction

Only a few low-mass X-ray binaries (LMXBs), systems where a compact object like a neutron star or a black hole accretes matter from a companion star via Roche lobe overflow, have been studied with polarimetric techniques to date (Charles et al. 1980; Dolan & Tapia 1989; Gliozzi et al. 1998; Hannikainen et al. 2000; Schultz et al. 2004; Brocksopp et al. 2007; Shahbaz et al. 2008; Russell & Fender 2008; Russell et al. 2011). Polarisation provides a powerful diagnostic tool to obtain information about geometrical and physical conditions of these systems, scattering properties of their accretion discs, or the presence of strong magnetic fields.

Most of the LMXB radiation is expected to be unpolarized. Optical light from LMXBs is in fact principally made of thermal black-body radiation from the accretion disc and the companion star, and does not possess any preferential direction of oscillation. Hydrogen in the disc is nevertheless in many cases totally ionised; for this reason, a significant (but small) linear polarisation (LP) is expected in the optical (Dolan 1984; Cheng et al. 1988) due to Thomson scattering of emitted unpolarised radiation with free electrons in the disc. This linear polarisation

component is usually almost constant for scattering in the nearly symmetrical accretion disc. If there are deviations from axial symmetry, some phase-dependent variations might be expected. Furthermore, radiation emitted from the accretion disc could interact via inverse Compton scattering with the electrons in a hot plasma corona that surrounds the disc itself (Haardt 1993). This phenomenon could induce high frequency polarisation.

Another possible and intriguing origin of significant polarisation is synchrotron emission, which arises from emission of a relativistic particle jet. Optically thin synchrotron radiation produces intrinsically linearly polarized light at a high level, up to ten per cent, especially in the near-IR (Russell & Fender 2008). Jets in X-ray binaries are expected to be linked to accretion (disc-jet coupling, Fender 2001b), and for this reason they have been principally observed in persistent systems or during the outbursts of transient LMXBs, especially if they contain a black hole. In the past few years, the evidence for jet emission during quiescence of LMXBs, containing both black holes and neutron stars, have been reported (Russell et al. 2006; Russell et al. 2007; Russell & Fender 2008; Baglio et al. 2013; Shahbaz et al. 2013). The detection of a high level of linear polarisation in the near-IR is for this reason considered the main route to assess for the emission of a relativistic jet.

Radiation from any source can also be polarised by the interaction with interstellar dust. This effect depends on the

<sup>★</sup> Based on observations made with ESO Telescopes at the La Silla Observatory under programme ID 080.D-0849(A).

wavelength as described by the Serkowski law (Serkowski et al. 1975), and must be accounted for in the analysis.

Transient LMXBs are generally faint objects in the optical; for this reason, only the brightest LMXBs have been observed in polarimetry. The majority of these studies regarded systems during outbursts or systems with BHs as compact object during quiescence.

In this paper, we report the results of the optical multi-band (*BVRI*) and infrared (*J*-band) polarimetric observations of the LMXB Cen X-4 during quiescence using the ESO 3.6 m telescope at La Silla and the Telescopio Nazionale *Galileo* (TNG) telescope, respectively. This is the first polarimetric study of a quiescent LMXB containing a NS.

Cen X-4 was discovered in 1969 during an X-ray outburst by the X-ray satellite Vela 5B (Conner et al. 1969). During a second outburst in 1979 the source was detected in the radio band (Hjellming 1979) as well, and its optical counterpart was identified with a blue star that had brightened by 6 mag to  $V = 13$  (Canizares et al. 1980). The companion star was classified at a later stage as a  $0.7 M_{\odot}$  K5–7 star (Shahbaz et al. 1993; Torres et al. 2002), which evolved to fill its  $\sim 0.6 R_{\odot}$  Roche lobe. The  $\sim 15.1$  h orbital period has been determined thanks to the optical light curve ellipsoidal variations (Cowley et al. 1988; Chevalier et al. 1989; McClintock & Remillard 1990). Cen X-4 is one of the brightest quiescent systems in the optical known to date ( $V = 18.7$  mag) and possesses a non-negligible disc component in the optical that contributes  $\sim 80\%$  in *B*,  $\sim 30\%$  in *V*,  $25\%$  in *R* and  $10\%$  in *I* (Shahbaz et al. 1993; Torres et al. 2002; D’Avanzo et al. 2005). Cen X-4 is at a distance of  $1.2 \pm 0.3$  kpc (Kaluzienski et al. 1980) and the interstellar absorption is low ( $A_V = 0.3$  mag). These characteristics make Cen X-4 an excellent candidate for polarimetric studies in quiescence.

Throughout the paper all the uncertainties are at 68% confidence level unless stated differently.

## 2. Optical polarimetry

The system Cen X-4 was observed on 11–12 March 2008 with the ESO 3.6 m telescope at La Silla, using the EFOSC2 instrument in polarimetric mode with the optical *BVRI* filters (4400 Å–7930 Å). The nights were clear with seeing  $\leq 1''$ . We carried out image reduction following standard procedures: subtraction of an averaged bias frame and division by a normalized regular flat frame. We performed all the flux measures thanks to accurate aperture photometry made with daophot (Stetson 1987) for all the objects in the field. The polarimetric calibration was performed against two polarimetric standard polarised and non-polarised stars provided by the FORS consortium based on commissioning data taken with FORS1<sup>1</sup>.

A Wollaston prism has been inserted in the optical path. The incident radiation was split into two simultaneous and orthogonally polarised ordinary and extraordinary beams (o- and e-beams). Thanks to a Wollaston mask, the different images do not overlap. The use of a rotating half wave plate (HWP) allowed us to take images at four different angles with respect to the telescope axis ( $\Phi_i = 22.5^\circ(i - 1)$ ,  $i = 0, 1, 2, 3$ ). Alternating the filters, a set of ten images of 90 s integration were obtained for each HWP angle for the *BVI* filters and a set of nine images for each angle of the *R*-band, divided between the two nights of observations, and covering about the 30% of the orbital period.

The normalised Stokes parameters  $Q$  and  $U$  for linear polarisation (LP) of the observed radiation are commonly evaluated starting from flux measures in both o- and e-beams ( $f^o$ ,  $f^e$ ) at just two orientation angles of the telescope’s axis ( $0^\circ$  and  $45^\circ$ ):

$$Q = \frac{f^o(0^\circ) - f^e(0^\circ)}{f^o(0^\circ) + f^e(0^\circ)}; \quad U = \frac{f^o(45^\circ) - f^e(45^\circ)}{f^o(45^\circ) + f^e(45^\circ)}. \quad (1)$$

Thanks to the rotating HWP, a higher accuracy measure of  $Q$  and  $U$  is possible, using the whole set of possible orientations. If  $\Phi_i$  are the HWP orientation angles defined as above,  $Q$  and  $U$  can be obtained from:

$$Q = \frac{F(\Phi_1) - F(\Phi_3)}{2}; \quad U = \frac{F(\Phi_2) - F(\Phi_4)}{2}, \quad (2)$$

where

$$F(\Phi_i) = \frac{f^o(\Phi_i) - f^e(\Phi_i)}{f^o(\Phi_i) + f^e(\Phi_i)}. \quad (3)$$

A first raw estimate of the observed polarisation degree  $P_{\text{obs}}$  and angle  $\theta$  can then be obtained as:

$$P_{\text{obs}} = (U^2 + Q^2)^{0.5} \quad (4)$$

$$\theta = 0.5 \tan^{-1}(U/Q). \quad (5)$$

Since the Stokes parameters statistics is not Gaussian (Wardle & Kronberg 1974; di Serego Alighieri 1998), the calculated values of linear polarisation have to be corrected for a bias factor. The real polarisation degree  $P$  can be obtained from:

$$P = P_{\text{obs}} \sqrt{1 - \left(\frac{\sigma_P}{P_{\text{obs}}}\right)^2}, \quad (6)$$

where  $\sigma_P$  is the rms error on the polarisation degree.

### 2.1. Averaged Stokes parameters for LP

We obtained the averaged (over all of the observations) Stokes parameters  $Q$  and  $U$  (Eq. (2)) in all of the filters analysed, for Cen X-4 and a selection of eight isolated and non-saturated reference stars, supposed to be unpolarised. A correction with respect to the average Stokes parameters measured for the reference field stars in each filter was then obtained for  $Q$  and  $U$  separately. This correction, which is small (at most 0.1%), supports our hypothesis that the reference stars are not polarised, and is crucial in order to eliminate most of the instrumental contribution to the Stokes parameters of the target. The same correction has been applied to the reference stars themselves. The errors on  $Q$  and  $U$  were found simply by propagating the photometric errors with the uncertainties obtained for the unpolarised field stars averaged Stokes parameters.

As shown in Fig. 1, the Stokes parameters evaluated for the reference stars and corrected as explained above form a cluster around 0 in each filter. The fact that the target might show different behaviour with respect to this selection of unpolarised stars can be due to higher interstellar absorption (if distance is larger than that of the stars), or to a real intrinsic polarisation component. This comparative method has been used for gamma-ray bursts afterglows (Covino et al. 1999) and for X-ray binaries (Dubus & Chaty 2006).

The only filters for which Cen X-4 lies at a  $\geq 3\sigma$  level from the weighted mean of the reference stars are the *V*- and *R*-bands, whereas in *B*- and *I*-bands the source’s Stokes parameters are comparable with those of the reference stars. To evaluate the

<sup>1</sup> <http://www.eso.org/sci/facilities/paranal/instruments/fors/inst/pola.html>

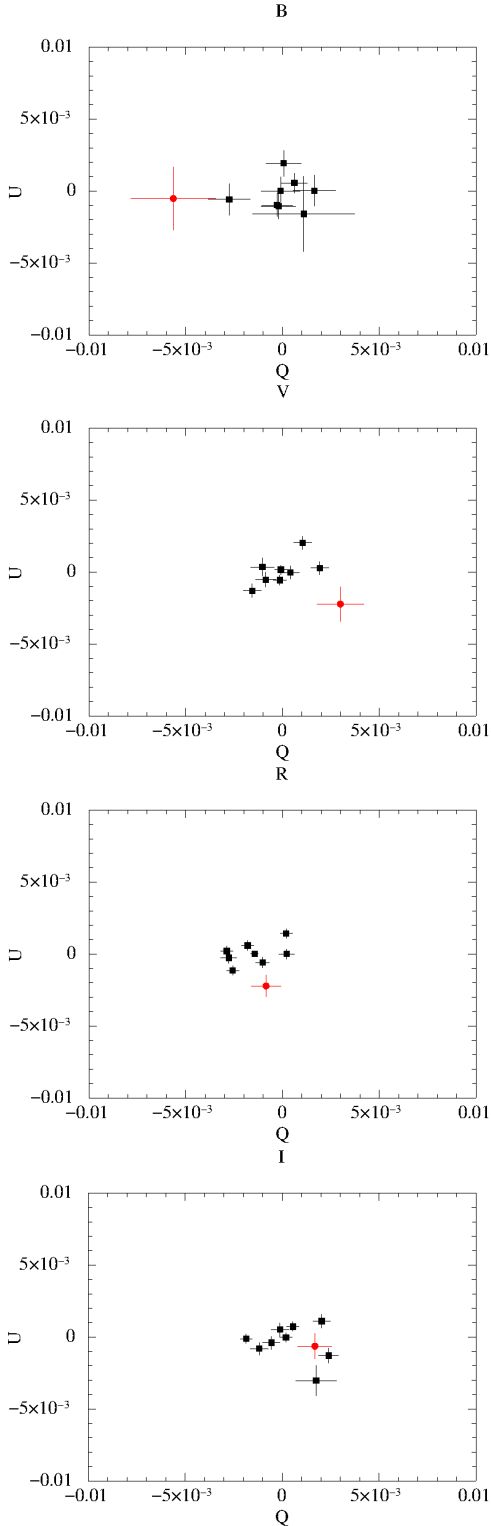


**Fig. 1.**  $U$  vs.  $Q$  for the averaged images of the four optical filters  $BVRI$ , for Cen X-4 (red dots) and for eight reference field stars (black squares). The represented Stokes parameters have been already corrected for the effect of instrumental polarisation, as described in Sect. 2.1.

polarisation degree  $P$ , one can use Eq. (4), with the correction reported in Eq. (6). This method is nevertheless not advised in case the rms error on  $P_{\text{obs}}$  is comparable to  $P_{\text{obs}}$  itself. In particular, in our case, the smallest obtained error bar for Cen X-4 corresponds to  $\sim 50\%$  of the measure, except for the  $I$ -band, where the signal-to-noise ratio (S/N) is higher. In this case, the

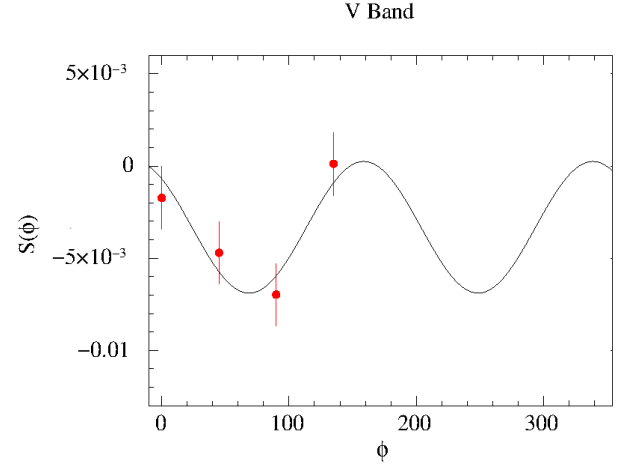


**Fig. 2.** Cosinusoidal  $V$ -band fit of  $S(\Phi)$  for Cen X-4.

best way to estimate  $P$  and the polarisation angle  $\theta$  is reported in the next section.

## 2.2. The $S$ parameter

The simple calculus proposed in Eq. (4) does not account for the possible interstellar polarisation and of Wollaston prism's imperfections. For this reason, it is necessary to apply a correction to the Stokes parameters obtained with Eq. (2), relying on polarimetric standard stars. Alternatively, it is possible to evaluate, for each HWP angle  $\Phi$  defined as in Sect. 2, a parameter  $S(\Phi)$  starting from the o- and e-fluxes of the target,  $f^o(\Phi)$  and  $f^e(\Phi)$ , and from the averaged ratio between o- and e-fluxes of some unpolarised field stars  $f_u^o(\Phi)$  and  $f_u^e(\Phi)$ . In particular, this parameter can be expressed as (di Serego Alighieri 1998; Covino et al. 1999):

$$S(\Phi) = \left( \frac{f^o(\Phi)/f^e(\Phi)}{\langle f_u^o(\Phi)/f_u^e(\Phi_i) \rangle} - 1 \right) / \left( \frac{f^o(\Phi)/f^e(\Phi)}{\langle f_u^o(\Phi)/f_u^e(\Phi) \rangle} + 1 \right). \quad (7)$$

This parameter can be regarded as the component of the normalised Stokes vector that describes LP along the direction selected by the HWP angle  $\Phi$ . The relation between  $S$ ,  $P$ , and  $\theta$  is given by:

$$S(\Phi) = P \cos 2(\theta - \Phi). \quad (8)$$

In this way, one can fit the function  $S(\Phi)$  with Eq. (8) and obtain  $P$ ,  $\theta$  and their errors from the semi-amplitude of the curve and from the  $x$ -value that corresponds to the first curve's maximum, respectively. With this method the measure of a polarimetric standard star becomes useless, since the parameter  $S$  is already normalised to the non-polarised reference stars, which all cluster around the same point of the plane ( $Q$ ,  $U$ ) in each filter. In particular, the so-obtained values should be automatically corrected for interstellar and instrumental effects, and do not need any bias correction (Eq. (6)). The sinusoidal fits of  $S(\Phi)$  for the  $V$ -band is reported in Fig. 2.

Adopting this method we derived the polarisation levels of Cen X-4 in the four optical bands. There only is a detection of polarisation different from 0 within  $1\sigma$  in the  $V$  and  $R$ -band. Since at least a  $3\sigma$  over zero polarisation degree would be an evidence of an intrinsic polarisation detection, we decided to quote the  $3\sigma$  upper limits in all bands (Table 1). As reported in Table 1, the  $3\sigma$  upper limit for the  $I$  band is really tightly constrained, because of the higher measured S/N with respect

**Table 1.** Values of the  $V$  and  $R$ -band detected polarisation degrees  $P$ , and  $BVRI$ -band  $3\sigma$  upper limits and polarisation angles for Cen X-4.

$B$	$V$	$R$	$I$
–	$0.36 \pm 0.18$	$0.19 \pm 0.16$	–
	$P$ (%)		
	$P$ ( $3\sigma$ upper limit)		
1.46%	0.90%	0.67%	0.46%
	$\theta$ ( $^\circ$ )		
$159.41^{+49.59}_{-51.42}$	$158.75^{+14.25}_{-15.75}$	$167.81^{+24.19}_{-25.81}$	$189.87 \pm 49.13$

**Notes.** The errors have been evaluated using contour plots in each band. In particular, to obtain the 68% c.l. we used  $\Delta\chi^2 = 2.3$  as requested for fits with two free parameters.

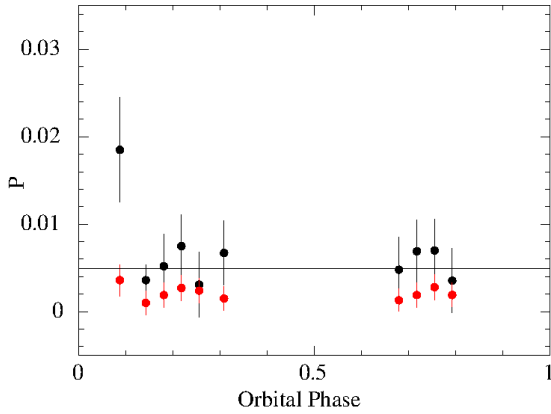


**Fig. 3.**  $V$ -band polarisation curve of Cen X-4 (black squares) and of one field star (red dots), with superimposed the linear fit to the data.

to the other bands. No evidence of a significant wavelength dependency of  $P$  is observed, since the polarisation measures in all bands are consistent with each other within  $2\sigma$ .

Following Serkowski et al. (1975), we were then able to evaluate the maximum expected interstellar contribution to the LP ( $P_{\max}$ ) of Cen X-4. In particular, we retrieved the empirical formula  $P_{\max} \leq 3A_V$ , according to which the maximum contribution to the LP for Cen X-4 due to interstellar effects should remain under the 0.9% level, consistently with our results.

### 2.3. Search for phase dependent variations of $P$

We obtained the values reported in Table 1 by summing all the images taken for each filter; this increased the S/N for our measurement, but let us loose all the information about possible orbital phase-correlated variations of  $P$ ,  $Q$  and  $U$ . In order to investigate the possible variability of the polarisation along  $P_{\text{orb}}$ , we analysed the single images calculating the orbital phases thanks to the precise ephemerides of Casares et al. (2007). Because of the large error bars, however, the data proved inconclusive.

We found the only variation from the linear fit to the data in all the analysed filters during the first epoch in the  $V$ -band (Fig. 3). In fact, at phase 0.1 (that is, when the companion star contribution is close to its minimum) we measured a polarisation degree of  $1.85\% \pm 0.60\%$ , i.e.  $2.3\sigma$  from the average.

However, we observed no similar features in the other bands, and furthermore this sudden increase in polarisation does not coincide with an increase or decrease of the observed flux. For these reasons, we conclude that we have observed an effect linked to photon statistics, and that any variability of polarisation

intrinsic to Cen X-4 is too weak to be detected from our dataset, with the relatively low S/N we have obtained in our observations.

## 3. Infrared polarimetry

The LMXB Cen X-4 was observed in IR ( $J$ -band,  $1.27 \mu\text{m}$ ) on 24 April 2007 with the TNG telescope at La Palma, equipped with the NICS instrument used in polarimetric mode. A set of 20 images of the field of 180 s integration each was obtained. A Wollaston prism was inserted in the grism wheel, which split incident radiation into four polarisation components ( $0^\circ$ ,  $45^\circ$ ,  $90^\circ$  and  $135^\circ$  with respect to the telescope's axis). These components were then re-imaged at different positions along the  $Y$ -axis.

We carried out image reduction by subtracting the sky background from each frame.

Because of a technical problem with the instrument derotator, only 25% of the images have been used for our purposes. We summed the selected images together to obtain a single image with an exposure time of 900 s. We made flux measures thanks to aperture photometry performed with daophot for all the objects in the field.

The normalised Stokes parameters  $Q$  and  $U$  have been calculated from<sup>2</sup>

$$Q = \frac{f(0^\circ) - f(90^\circ)}{f(0^\circ) + f(90^\circ)}; \quad U = \frac{f(45^\circ) - f(135^\circ)}{f(45^\circ) + f(135^\circ)}, \quad (9)$$

whereas the polarisation degree  $P$  can be obtained from Eq. (4).

### 3.1. Results

We selected a sample of four isolated and supposed to be unpolarised stars in the field, in a region of the image as close as possible to the target, to compare with Cen X-4, and we calculated  $Q$  and  $U$  for all of them. As we did for optical data, we represented the Stokes parameters in the  $Q - U$  plane and we observed that Cen X-4 was comparable to the field stars, which all cluster around a common value, corresponding to the possible instrumental polarisation contribution. In Fig. 4, we reported the  $Q$  vs.  $U$  plot for Cen X-4 and the four reference stars, with all the parameters corrected for the weighted mean of the field stars Stokes parameters.

Due to the large error bars measured for both the target and the field stars, we decided to evaluate a  $3\sigma$  upper limit to the  $J$ -band polarisation directly. We performed a Monte Carlo simulation starting from the values of  $Q$  and  $U$  of Cen X-4 corrected for the average  $Q$  and  $U$  measured for the field stars, and we obtained an upper limit to  $P$  of  $\sim 6\%$  within  $3\sigma$  (the upper limit is of  $\sim 4\%$  at a  $1\sigma$  confidence level).

## 4. Discussion

### 4.1. Jets in quiescence?

As stated in Russell et al. (2011), a polarimetric signature of the emission of a relativistic particles jet in LMXB is theoretically detectable both in the infrared and in the optical. In black hole and neutron star X-ray binaries, the linear polarisation degree of the emitted radiation is expected not to exceed a few %, with evidence of variability on short time-scales. This suggests that a tangled and turbulent (no more than partially ordered) magnetic field is generally present at the base of the jet (there was a

<sup>2</sup> [http://www.tng.iac.es/instruments/nics/files/pol\\_obs\\_v03.pdf](http://www.tng.iac.es/instruments/nics/files/pol_obs_v03.pdf)

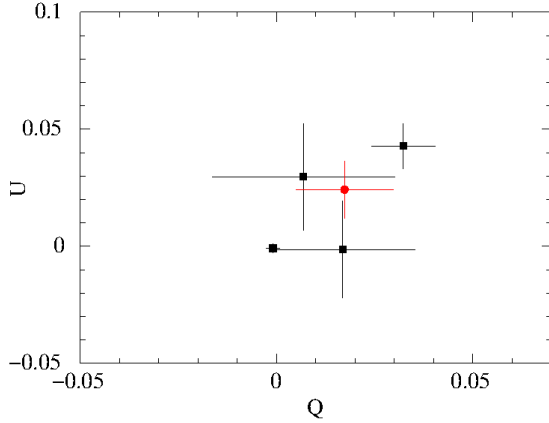


**Fig. 4.**  $U$  vs.  $Q$  for the  $J$ -band observations, for Cen X-4 (red dot) and for four isolated reference stars (black squares). All the Stokes parameters values have been corrected for the weighted mean of  $Q$  and  $U$  of the field stars.

unique detection of a highly ordered magnetic field in an X-ray binary for the persistent system Cyg X-1, [Russell & Shahbaz 2014](#)). Something similar also seems to happen in the case of compact jets from active galactic nuclei (AGN), in particular in gigahertz peaked-spectrum sources where the low level of polarisation (1–7%) measured in the optically thin regime is interpreted with the presence of a tangled magnetic field ([O’Dea 1998](#)). Also the flat-spectrum radio jets of AGN usually possess a low polarisation degree (1–5%), similar to the radio jets of X-ray binaries, suggesting tangled and helical magnetic fields ([Helmboldt et al. 2007](#); [Perlman et al. 2011](#)).

For Cen X-4, the measured degree of linear polarisation averaged over all observations is  $\lesssim 1.5\%$  in the optical  $BVRI$  filters, and  $\lesssim 6\%$  in the  $J$ -band within  $3\sigma$  (Table 1). Under the hypothesis that neutron star X-ray binaries could exhibit a similar behaviour to that of black hole X-ray binaries in terms of jet emission, these upper limits are effectively consistent with the possible emission of a jet with low polarisation degrees possibly linked to the tangled and non-ordered structure of the magnetic field in a region close to the one where the jet is launched. However, no observational constraints of how tangled neutron star jets magnetic fields are exist to date.

A possible way to search for the presence of the relativistic particle jet is to observe the spectral energy distribution (SED) of the system Cen X-4, as stated in [Fender \(2001a\)](#). In fact, in case of jet emission, an excess in the SED in the range of frequencies where the synchrotron emission gives its maximum contribution (near-IR) is expected. The emission in this case would be characterised by an optically thick synchrotron radio spectrum (that corresponds to  $\alpha \geq 0$ , where  $\alpha$  is the spectral index and the flux density  $F_\nu$  is proportional to  $\nu^\alpha$ ), which should switch to an optically thin synchrotron spectrum at shorter wavelengths (i.e.  $\alpha \approx -0.6$ ). The break frequency is expected to fall in the mid-infrared ([Fender 2001b](#); [Corbel & Fender 2002](#); [Gallo et al. 2007](#); [Migliari et al. 2007](#); [Pe’er & Casella 2009](#); [Migliari et al. 2010](#); [Rahoui et al. 2011](#); [Gandhi et al. 2011](#)).

We thus built the SED of the system (Fig. 5), starting from IR data taken from the WISE All Sky and 2MASS catalogues<sup>3</sup> and from the optical  $V$ - and  $B$ -band data obtained from [Cackett et al. \(2013\)](#) during quiescence for Cen X-4. The fluxes values considered for the SED are reported in Table 2.

<sup>3</sup> [http://irsa.ipac.caltech.edu/workspace/TMP\\_qLHgEi\\_32284/Gator/irsa/32533/tbview.html](http://irsa.ipac.caltech.edu/workspace/TMP_qLHgEi_32284/Gator/irsa/32533/tbview.html)

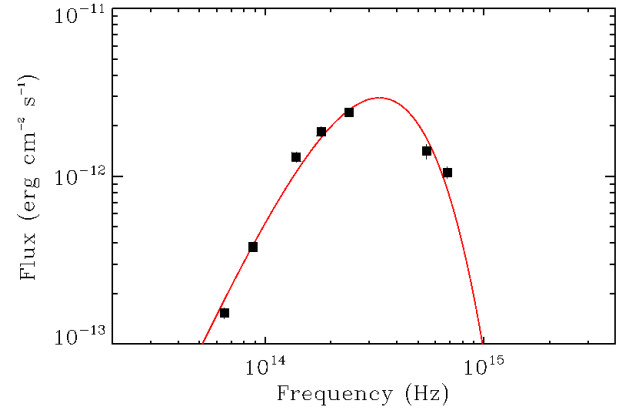


**Fig. 5.** Spectral energy distribution of Cen X-4 built starting from IR archival data and from the optical fluxes obtained by [Cackett et al. \(2013\)](#). The three datasets are not contemporary. Superimposed, the fit of the data with a black body of an irradiated star.

**Table 2.** IR and optical dereddened fluxes obtained from the WISE and 2MASS catalogues and from [Cackett et al. \(2013\)](#), used to build the multi-wavelength SED of Cen X-4 (Fig. 5).

Band	Flux (erg cm <sup>-2</sup> s <sup>-1</sup> )
$W_2$ WISE ( $\lambda = 4.6 \mu\text{m}$ )	$(1.53 \pm 0.12) \times 10^{-13}$
$W_1$ WISE ( $\lambda = 3.4 \mu\text{m}$ )	$(3.79 \pm 0.13) \times 10^{-13}$
$K$ 2MASS ( $\lambda = 2.16 \mu\text{m}$ )	$(1.30 \pm 0.10) \times 10^{-12}$
$H$ 2MASS ( $\lambda = 1.66 \mu\text{m}$ )	$(1.85 \pm 0.13) \times 10^{-12}$
$J$ 2MASS ( $\lambda = 1.23 \mu\text{m}$ )	$(2.40 \pm 0.13) \times 10^{-12}$
$V$ ( <a href="#">Cackett et al. 2013</a> , $\lambda = 5468 \text{ \AA}$ )	$(1.41 \pm 0.14) \times 10^{-12}$
$B$ ( <a href="#">Cackett et al. 2013</a> , $\lambda = 4392 \text{ \AA}$ )	$(1.05 \pm 0.09) \times 10^{-12}$

As shown in Fig. 5, the SED is consistent with a single black-body contribution, likely due to the irradiated companion star (a similar result was obtained through the study of the correlations between UV and X-ray variability; [Bernardini et al. 2013](#)). No IR excess has been observed. In particular, a power-law fit ( $I_\nu \propto \nu^\alpha$ ) of the lower frequencies data reported an index  $\alpha$  of  $1.81 \pm 0.14$ , which is exactly opposite from what is expected for an IR excess ( $\alpha \leq 0$ ), and on the contrary, is typical of a low frequency black-body approximation ( $I_\nu \propto \nu^2$ ). In particular, the fit of the SED with a black-body with fixed radius (corresponding to the Roche lobe dimension,  $0.6 R_\odot$ ) reported a black-body temperature of  $4050 \pm 30$  K, which is consistent with a K spectral type main-sequence star, and an irradiation luminosity of  $4.5 (\pm 5.5) \times 10^{32}$  erg/s. This is consistent with the X-ray luminosity reported in [Campana et al. \(2004\)](#). The non-detection of IR excess cannot however totally exclude the emission of a jet that could theoretically exist in Cen-X4 in quiescence, but it may only be detectable at radio frequencies.

If we hypothesize the effective emission of a jet from Cen X-4, we should expect at most a polarisation degree of a few % in the optical (for instance 5%), which is typical of X-ray binaries jets with tangled magnetic fields. In order to obtain such a polarisation degree, we thus considered the most constraining  $3\sigma$  upper limit we obtained in our analysis (that is  $P < 0.5\%$  in the  $I$ -band) and evaluated the maximum possible contribution of the relativistic jet to the total  $I$ -band flux to be at most 10%. This upper limit to the jet emission is fairly constraining and is totally in agreement with the blue  $IR$  SED shown in Fig. 5.

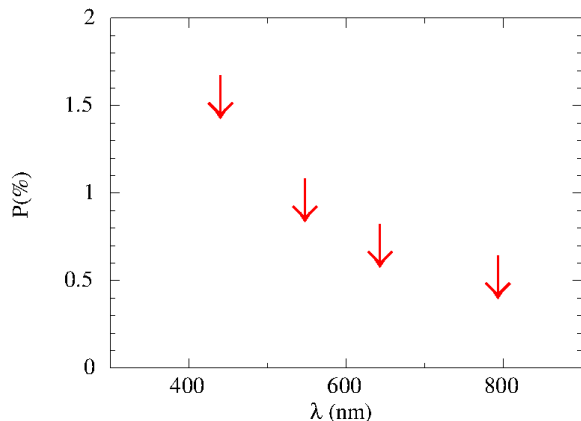


**Fig. 6.** Polarisation degree  $3\sigma$  upper limits trend with respect to the wavelength of the four optical filters analysed, *BVRI*.

Relativistic particles jets have been detected in some persistent neutron star X-ray binaries in IR and radio frequencies (i.e. [Migliari et al. 2006](#)), but there has never been a detection during quiescence. In particular, [Migliari et al. 2006](#) predicted a steeper radio/X-ray correlation in neutron star X-ray binaries compared to black hole X-ray binaries, which would imply the possible emission of very faint jets from quiescent neutron stars, in accordance with our result.

#### 4.2. Thomson scattering

As explained in Sect. 1, scattering of radiation with electrons in the ionised disc can result in linear polarisation. The polarisation degree  $P$  that is derived from this mechanism is expected to increase as a function of decreasing wavelength and not to be more than a few per cent ([Brown et al. 1978](#); [Dolan 1984](#)). In our case, the measured average polarisation degrees in the four filters never exceed the 1% level, and for this reason could be consistent with the low polarisation degree expected in case of Thomson scattering with the free electrons in the disc. Unfortunately, the low S/N of our measures do not allow us to verify the expected increasing trend of  $P$  with decreasing wavelength (Fig. 6).

Furthermore, scattering should also produce a linear polarisation degree that varies on time-scales of the orbital period ([Kemp & Barbour 1983](#); [Dolan & Tapia 1989](#); [Gliozzi et al. 1998](#)). In our case, we observed an almost constant trend of the polarisation degrees in the four analysed filters. The only epoch that possesses a polarisation degree significantly higher than the average is in the *V*-band at phase 0.1. In this epoch, the companion star's contribution is at its minimum, i.e. the accretion disc should be mostly responsible for the observed variation. This fact grows in interest in light of the Thomson scattering hypothesis. Nevertheless, the absence of similar behaviours in consecutive bands (and time), which in contrast showed almost constant  $P$ , let this observation become less intriguing. We conclude that if there was a variation of  $P$  with the system's orbital phase, we were not able to detect it, because of the large error bars, often comparable to the potential oscillation's semi-amplitudes.

## 5. Conclusions

In this work, we presented the results of an optical (*BVRI*) and infrared (*J*) polarimetric study on the LMXB Cen X-4 during quiescence, based on observations obtained in 2008 and 2007, respectively.

We were searching for an intrinsic component of linear polarisation in the optical and IR for this source. We obtained a low polarisation degree  $3\sigma$  upper limit in each optical filter, with the highest value in the *B*-band ( $P_B \leq 1.46\%$ ) and lowest in the *I*-band, where  $P$  is consistent with 0 within  $1\sigma$ . A  $3\sigma$  upper limit to the linear polarisation of 6% is obtained in the *J*-band.

We built the SED of Cen X-4 from literature data, observing that it can be fitted by the only black body of the irradiated companion star. Assuming a typical expected polarisation degree of at most 5% for a NS X-ray binary jet with tangled magnetic field, our *I*-band upper limit on the linear polarisation implies that the contribution from a possible jet should be relatively low ( $\lesssim 10\%$ ) in terms of flux. This is in agreement with the non-detection of an infrared excess in the SED of Cen X-4.

We detected no variations correlated with the orbital period of the system and, because of the large error bars caused by the low S/N, it was not possible to be conclusive on a possible increasing trend of  $P$  with decreasing wavelength, which should support the possibility of Thomson scattering of the radiation with accretion disc particles. Observations with larger diameter telescopes (8 m class) would provide smaller uncertainties for the Stokes parameters (in particular in the *B*-band, where Cen X-4 is fainter). This will be crucial to best investigate possible phase-orbital correlated variations of  $P$  and its wavelength trend to assess the origin of polarisation for Cen X-4.

*Acknowledgements.* We thank the anonymous referee for useful comments and suggestions. M.C.B. acknowledges P. M. Pizzochero for supportive discussions and the INAF-Osservatorio Astronomico di Brera for kind hospitality during her master thesis. P.D.A. acknowledges L. Monaco, E. Matamoros and A. Ederoclitte for their support during his observing run in La Silla. P.D.A. acknowledges V. Lorenzi and the TNG staff for their support in carrying out the NICS observations in service mode.

## References

- Baglio, M. C., D'Avanzo, P., Muñoz-Darias, T., Breton, R. P., & Campana, S. 2013, *A&A*, 559, A42
- Bernardini, F., Cackett, E. M., Brown, E. F., et al. 2013, *MNRAS*, 436, 2465
- Brocksopp, C., Miller-Jones, J. C. A., Fender, R. P., & Stappers, B. W. 2007, *MNRAS*, 378, 1111
- Brown, J. C., McLean, I. S., & Emslie, A. G. 1978, *A&A*, 68, 415
- Cackett, E. M., Brown, E. F., Degenaar, N., et al. 2013, *MNRAS*, 433, 1362
- Campana, S., Israel, G. L., Stella, L., Gastaldello, F., & Mereghetti, S. 2004, *ApJ*, 601, 474
- Canizares, C. R., McClintock, J. E., & Grindlay, J. E. 1980, *ApJ*, 236, L55
- Casares, J., Bonifacio, P., González Hernández, J. I., Molaro, P., & Zoccali, M. 2007, *A&A*, 470, 1033
- Charles, P. A., Thorstensen, J. R., Bowyer, S., et al. 1980, *ApJ*, 237, 154
- Cheng, F. H., Shields, G. A., Lin, D. N. C., & Pringle, J. E. 1988, *ApJ*, 328, 223
- Chevalier, C., Ilovaisky, S. A., van Paradijs, J., Pedersen, H., & van der Klis, M. 1989, *A&A*, 210, 114
- Conner, J. P., Evans, W. D., & Belian, R. D. 1969, *ApJ*, 157, L157
- Corbel, S., & Fender, R. P. 2002, *ApJ*, 573, L35
- Covino, S., Lazzati, D., Ghisellini, G., et al. 1999, *A&A*, 348, L1
- Cowley, A. P., Hutchings, J. B., Schmidtke, P. C., et al. 1988, *AJ*, 95, 1231
- D'Avanzo, P., Campana, S., Casares, J., et al. 2005, *A&A*, 444, 905
- di Serego Alighieri S. 1998, in *Instrumentation for Large Telescopes*, ed. J. M. Rodríguez. Espinosa (Cambridge University Press), 287
- Dolan, J. F. 1984, *A&A*, 138, 1
- Dolan, J. F., & Tapia, S. 1989, *PASP*, 101, 1135
- Dubus, G., & Chaty, S. 2006, *A&A*, 458, 591
- Fender, R. 2001a, in *The Second National Conference on Astrophysics of Compact Objects*, 14
- Fender, R. P. 2001b, *MNRAS*, 322, 31
- Gallo, E., Migliari, S., Markoff, S., et al. 2007, *ApJ*, 670, 600
- Gandhi, P., Blain, A. W., Russell, D. M., et al. 2011, *ApJ*, 740, L13
- Gliozzi, M., Bodo, G., Ghisellini, G., Scaltriti, F., & Trussoni, E. 1998, *A&A*, 337, L39

- Haardt, F. 1993, *ApJ*, 413, 680
- Hannikainen, D. C., Hunstead, R. W., Campbell-Wilson, D., et al. 2000, *ApJ*, 540, 521
- Helmboldt, J. F., Taylor, G. B., Tremblay, S., et al. 2007, *ApJ*, 658, 203
- Hjellming, R. M. 1979, *IAU Circ.*, 3369, 1
- Kaluzienski, L. J., Holt, S. S., & Swank, J. H. 1980, *ApJ*, 241, 779
- Kemp, J. C., & Barbour, M. S. 1983, *ApJ*, 264, 237
- McClintock, J. E., & Remillard, R. A. 1990, *ApJ*, 350, 386
- Migliari, S., Tomsick, J. A., Maccarone, T. J., et al. 2006, *ApJ*, 643, L41
- Migliari, S., Tomsick, J. A., Markoff, S., et al. 2007, *ApJ*, 670, 610
- Migliari, S., Tomsick, J. A., Miller-Jones, J. C. A., et al. 2010, *ApJ*, 710, 117
- O'Dea, C. P. 1998, *PASP*, 110, 493
- Pe'er, A., & Casella, P. 2009, *ApJ*, 699, 1919
- Perlman, E. S., Adams, S. C., Cara, M., et al. 2011, *ApJ*, 743, 119
- Rahoui, F., Lee, J. C., Heinz, S., et al. 2011, *ApJ*, 736, 63
- Russell, D. M., & Fender, R. P. 2008, *MNRAS*, 387, 713
- Russell, D. M., & Shahbaz, T. 2014, *MNRAS*, 438, 2083
- Russell, D. M., Fender, R. P., Hynes, R. I., et al. 2006, *MNRAS*, 371, 1334
- Russell, D. M., Fender, R. P., & Jonker, P. G. 2007, *MNRAS*, 379, 1108
- Russell, D. M., Casella, P., Fender, R., et al. 2011, *Proc. Science*, PoS(HTRA-IV), 009
- Schultz, J., Hakala, P., & Huvelin, J. 2004, *Baltic Astron.*, 13, 581
- Serkowski, K., Mathewson, D. S., & Ford, V. L. 1975, *ApJ*, 196, 261
- Shahbaz, T., Naylor, T., & Charles, P. A. 1993, *MNRAS*, 265, 655
- Shahbaz, T., Fender, R. P., Watson, C. A., & O'Brien, K. 2008, *ApJ*, 672, 510
- Shahbaz, T., Russell, D. M., Zurita, C., et al. 2013, *MNRAS*, 434, 2696
- Stetson, P. B. 1987, *PASP*, 99, 191
- Torres, M. A. P., Casares, J., Martínez-Pais, I. G., & Charles, P. A. 2002, *MNRAS*, 334, 233
- Wardle, J. F. C., & Kronberg, P. P. 1974, *ApJ*, 194, 249